The Dlx5 homeodomain gene is essential for normal olfactory development and connectivity in the mouse.

Available online at www.sciencedirect.com
SCIENCE DIRECT®
ACADEMIC PRESS
Molecular and Cellular Neuroscience 22 (2003) 530–543
MCN Molecular and Cellular Neuroscience
www.elsevier.com/locate/ymcne

The *Dlx5* homeodomain gene is essential for olfactory development and connectivity in the mouse

Giovanni Levi,[a,b] Adam C. Puche,[c] Stefano Mantero,[b] Ottavia Barbieri,[d] Sonya Trombino,[b] Laura Paleari,[b] Aliana Egeo,[e] and Giorgio R. Merlo[e,*,1]

[a] *Laboratoire de Physiologie Général et Comparée, CNRS, UMR 8572, Museum National d'Histoire Naturelle, Paris, France*
[b] *Laboratory of Molecular Morphogenesis, National Cancer Institute IST, Genoa, Italy*
[c] *Department of Anatomy and Neurobiology, University of Maryland, Baltimore, MD, USA*
[d] *Department of Oncology, Biology and Genetics, University of Genoa-IST, Genoa, Italy*
[e] *Dulbecco Telethon Institute-DTI, Centro Biotecnologie Avanzate, Largo R. Benzi 10, 16132 Genoa, Italy*

Received 21 August 2002; revised 16 November 2002; accepted 20 November 2002

Abstract

The *distalless*-related homeogene *Dlx5* is expressed in the olfactory placodes and derived tissues and in the anterior-basal forebrain. We investigated the role of *Dlx5* in olfactory development. In $Dlx5^{-/-}$ mice, the olfactory bulbs (OBs) lack glomeruli, exhibit disorganized cellular layers, and show reduced numbers of TH- and GAD67-positive neurons. The olfactory epithelium in $Dlx5^{-/-}$ mice is composed of olfactory receptor neurons (ORNs) that appear identical to wild-type ORNs, but their axons fail to contact the OBs. We transplanted $Dlx5^{-/-}$ OBs into a wild-type newborn mouse; wild-type ORN axons enter the mutant OB and form glomeruli, but cannot rescue the lamination defect or the expression of TH and GAD67. Thus, the absence of *Dlx5* in the OB does not per se prevent ORN axon ingrowth. In conclusion, *Dlx5* plays major roles in the connectivity of ORN axons and in the differentiation of OB interneurons.

Introduction

Olfactory receptor neurons (ORNs) form synapses with dendrites of second-order neurons within the glomeruli of the olfactory bulb (OB). Recent studies have demonstrated a high specificity between ORN axons and their target site. Axons from ORNs expressing the same odorant receptor gene sort and target glomeruli in topographically fixed locations (Buck, 2000; Mombaerts et al., 1996; Vassar et al., 1994; Wang et al., 1998).

Little is known about the cellular and molecular mechanisms governing development of the olfactory system, glomerulus formation, and ORN axon guidance. Several surface receptors and adhesion molecules have been implicated (Key, 1998; Lin and Ngai, 1999), among which are the odorant receptors (Mombaerts et al., 1996; Wang et al., 1998), semaphorins/neuropilins (Giger et al., 1998; Pasterkamp et al., 1999; Williams-Hogarth et al., 2000), Eph/Ephrins (Gao et al., 2000; St. John et al., 2000), netrin/DCC (Gad et al., 1997; Shu et al., 2000), Slit/Robo (Li et al., 1999; Wu et al., 1999), neural cell adhesion molecule (Treloar et al., 1997), Galectin-1 (Puche et al., 1996; Tenne-Brown et al., 1998), and the low-affinity neurotrophin receptor (Tisay et al., 2000). Transcription factors are also involved in this process. In the *small eye* mice harboring a mutation of *Pax6*, the olfactory placodes fail to form, resulting in the absence of ORNs (Anchan et al., 1997; Brunjes et al., 1998; Lopez-Mascaraque et al., 1998). While initial reports suggested the complete absence of OBs, a residual OB is indeed present (Lopez-Mascaraque et al., 1998). A second mutation, *extra toe*, is the result of a deletion of *Gli3* (Schimmang et al., 1992). In these mutants, the OBs are absent, although the olfactory epithelium (OE) is present and the ORN axons project to the location of the absent bulb (Franz, 1994). *Dlx* genes are the mammalian

* Corresponding author. Fax: +39-02-26422660.
E-mail address: gmerlo@dti.telethon.it (G.R. Merlo).
[1] Present address: CNR-ITB, Via Fratelli Cervi 93, 20090 Segrate (Milan) Italy.

1044-7431/03/$ – see front matter © 2003 Elsevier Science (USA). All rights reserved.
doi:10.1016/S1044-7431(02)00041-6

homologues of *Drosophila distalless*, encode for transcription factors with similar in vitro DNA binding properties (Liu et al., 1997), and are expressed in limb buds, craniofacial., mesenchyme, and restricted areas of the forebrain (Acampora et al., 1999; Bulfone et al., 1993a, 1993b; Merlo et al., 2000; Qui et al., 1997; Porteus et al., 1994; Robinson and Mahon, 1994). *Dlx1* and *Dlx2* are also expressed by interneurons of the OB and their combined disruption results in loss of GABAergic and dopaminergic neurons (Anderson et al., 1997; Bulfone et al., 1998). However, in these mice ORN axons reach the appropriate locations in the OB. *Dlx5* and *Dlx6* are expressed from early stages in the brain areas precursor to the OB and olfactory tubercle and in the ganglionic eminence (Simeone et al., 1994). Unlike *Dlx1* and *Dlx2*, *Dlx5* is also expressed early in anterior/lateral nonneural embryonic ectoderm, the presumptive territory of the olfactory placode (Yang et al., 1998).

We show here a unique olfactory phenotype in which the OE and OB of *Dlx5* null mice are present but no axonal connections are formed. Our data indicate that *Dlx5* plays a major role in the ability of ORN axons to reach the bulb and form glomeruli and in the organization and differentiation of cell layers in the OB.

Results

The olfactory epithelium in Dlx5 null mice

Dlx5 is expressed in the embryonic ectoderm anterior and lateral to the neural plate as early as E7 during development (Yang et al., 1998). These neural plate regions are precursors to the ventral cephalic epithelium and the olfactory placode. Expression of *Dlx5* is maintained throughout early embryonic stages in olfactory placode derivatives (Acampora et al., 1999). Using the *LacZ* reporter as a marker for *Dlx5* expression, we extended this analysis through P0 mice. *Dlx5/LacZ* is expressed throughout the OE lining the nasal cavity, and in the vomeronasal organ at all embryonic stages examined and at birth (Fig. 1, and data not shown). The nasal cavities of *Dlx5* null mutants are severely reduced in size and turbinates fail to develop (Acampora et al., 1999; Depew et al., 1999). The OE lining *Dlx5* null nasal cavities is on average two-thirds the normal thickness (Figs. 2D, 2H). The vomeronasal organ is also reduced in size and often fails to close.

ORNs of $Dlx5^{-/-}$ mice were characterized by examining the expression of several markers, including: (1) OMP, a marker for mature ORNs whose expression begins around E14.5, (2) N-CAM, a general neural marker, (3) PSA-N-CAM, an immature glycoform of N-CAM, (4) Emx1, a homeobox protein present in early ORN axons, and (5) calretinin, a calcium-binding protein expressed in mature ORNs beginning at E14.5 (Bastianelli and Pochet, 1994; Briata et al., 1996; Keller and Margolis, 1975; Margolis, 1972). At E16.5 and P0 all these proteins were detected in the $Dlx5^{-/-}$ OE, showing a distribution similar to that of normal OE (Figs. 2D, 2H). In particular, by late embryonic/early postnatal stages the number of cells expressing OMP and calretinin in the OE had not significantly changed between mutants and normal mice (Figs. 2C, 2D, 2G, 2H). At E14.5 both OMP and calretinin begin to be expressed in normal ORNs. At this stage, in $Dlx5^{-/-}$ OE expression of both OMP and calretinin was absent (Figs. 2B, 2F). These results indicate a delayed onset of expression of these ORN-specific markers.

Olfactory ensheathing cells originate from the olfactory placodes and accompany the ORN axons through the nasal mesenchyme (Chuau and Au, 1991; Norgren et al., 1992). These cells might play an important role in axonal extension, pathfinding, and target recognition (Ramon-Cueto and Avila, 1998). Olfactory Schwann cells can be detected by immunostaining for S100 protein and are normally found along the olfactory and vomeronasal nerves and in the nerve layer of the OB. In $Dlx5^{-/-}$ animals S100 immunoreactivity is absent in the OB nerve layer (data not shown). Thus, in $Dlx5^{-/-}$ animals S100-positive ensheathing cells remain associated with ORN axons and do not migrate de novo to the OB. In addition to the ensheathing cells, antibodies for S100 also stain a subpopulation of CNS astrocytes that was equally present in normal and in $Dlx5^{-/-}$ OB.

The organization of the basement membrane underlying the OE and at the border of the OB was analyzed by immunohistochemistry for laminin. At E13.5 laminin expression in the basement membrane surrounding the OB becomes fenestrated to allow for ORN axon penetration (Gong and Shipley, 1996; Treloar et al., 1996). In $Dlx5^{-/-}$ embryos, laminin staining in the OE basement membrane, blood vessels, and meninges was indistinguishable from that of the normal embryos (data not shown).

ORN axons in $Dlx5^{-/-}$ mice do not contact the OB

To visualize the trajectory of ORN projections in normal and $Dlx5^{-/-}$ embryos, we stained sections of mouse embryos at various stages (E11.5–E18.5) for the ORN-specific markers OMP, Emx1, calretinin, and GAP43 (Bastianelli and Pochet, 1994; Briata et al 1996; Keller and Margolis, 1975; Margolis, 1972). All of these proteins can be detected in the neurites of the developing olfactory and vomeronasal nerves beginning at different stages: OMP and calretinin appear around E15 while GAP43 is detectable from E12 and is used to visualize early neurites. In serial sections of $Dlx5^{-/-}$ embryos at E12.5, GAP43-positive neurites were observed. These appeared to be sparse, disoriented, and not contacting the OB, as compared with sections of $Dlx5^{+/-}$ embryos in which GAP43-positive neurites form a neuropile and reach the anterior forebrain (Figs. 3A, 3B). With all the markers used and at all developmental stages examined a physical connection between the olfactory and vomeronasal nerves and the OB has never been observed. In $Dlx5^{-/-}$ mice axons expressing OMP, Emx1, and calretinin extend

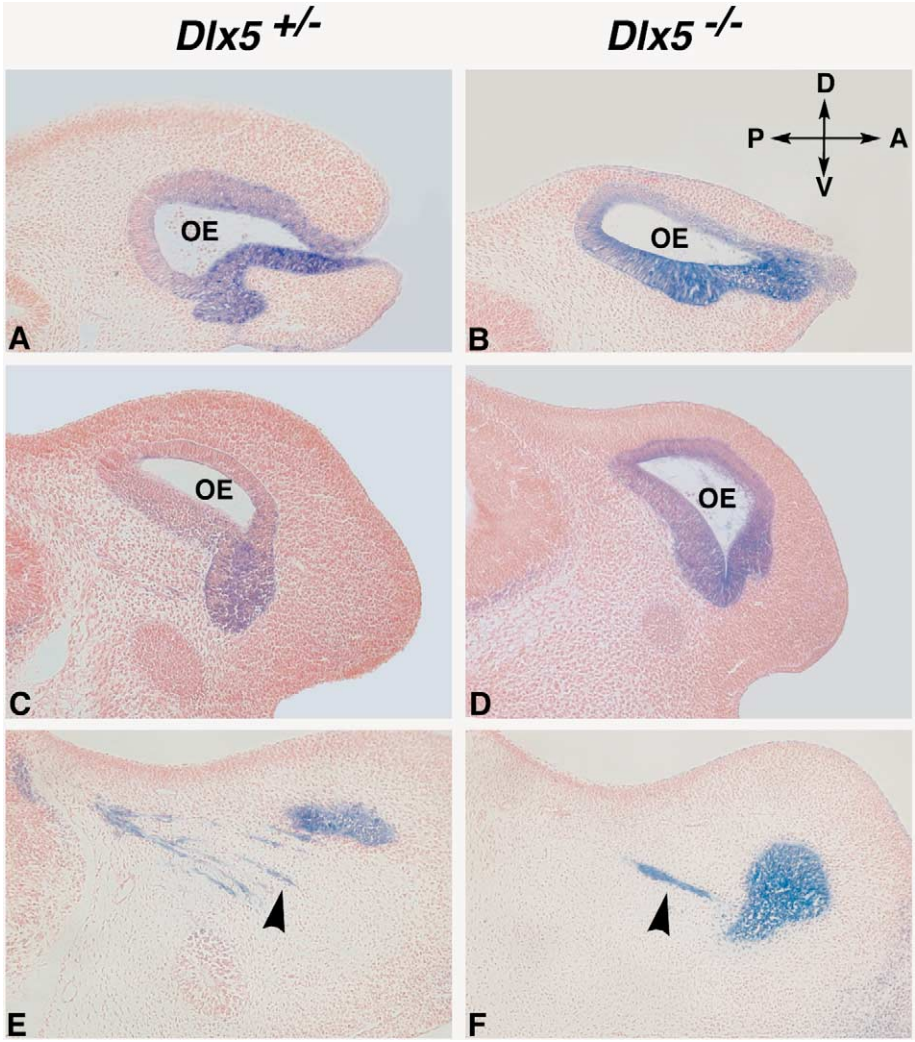

Fig. 1. Histology of the nasal region of *Dlx5*$^{-/-}$ mice. Longitudinal sections of E11.5 (A,B), E12.5 (C,D), and E13.5 (E,F) embryos stained with X-gal. Sections in (A)–(D) reveal *LacZ* expression in the epithelium of the nasal cavity; sections in (E) and (F) are chosen to show *LacZ* expression in olfactory and vomeronasal nerve bundles (black arrowheads). The orientation is indicated in (B). Panels on the left are from *Dlx5*$^{+/-}$ animals; panels on the right are from *Dlx5*$^{-/-}$ animals. OE, olfactory epithelium.

from the OE into the lamina propria underlying the OE and course toward the forebrain, but never reach the OB (see Emx1 staining at E14.5, Figs. 3C, 3D). The severity of this phenotype varies between individual mutant mice. At P0 the phenotype ranges from a few axon bundles confined in the lamina propria to more numerous ORN axon fascicles that cross the cribriform plate. In the latter cases the fibers form a neuroma adjacent to the OB (Fig. 3F). Consistent with the failure of ORN neurites to connect, absence of glomeruli is observed (Figs. 3F, 3H, 4J). To further confirm this finding, OBs from normal and *Dlx5*$^{-/-}$ mice were immunostained for Emx1, OMP, and calretinin. All these proteins are normally detected in the external nerve layer of the OB. In *Dlx5*$^{-/-}$ OBs none of these marker can be detected, indicating that the ORN axon component is missing (Figs. 5J, 5K, and data not shown).

Histological analysis can detect single ORN axons if the appropriate marker is expressed; however, it is possible that ORN axons not expressing these markers might contact the OB in *Dlx5*$^{-/-}$ mice. To rule out this possibility, we evaluated the trajectory of olfactory nerves (ONs) using the lipophilic fluorochrome DiI as a tracer followed by serial sectioning of the entire head (Figs. 3I. and 3II.). In *Dlx5*$^{-/-}$ specimens no fluorescent fibers can be seen entering the OB, whereas in the normal heads labeled axons are present throughout the entire nerve fiber and glomerular layers of the bulb (Figs. 3J–3L). Consistent with the reduced size of their nasal cavities, DiI-labeled ONs in *Dlx5*$^{-/-}$ are less numerous and the fascicles smaller. In the few *Dlx5* null animals in which ORN axons cross the cribriform plate, these axons always remain outside the OB, do not cross the meninges or enter the brain, and bend caudally and ventrally to the OB (Figs. 3K, 3L). Taken together, all these results indicate that a common feature of *Dlx5* null mice is the absence of the OE-to-OB connection, although the axons are able to

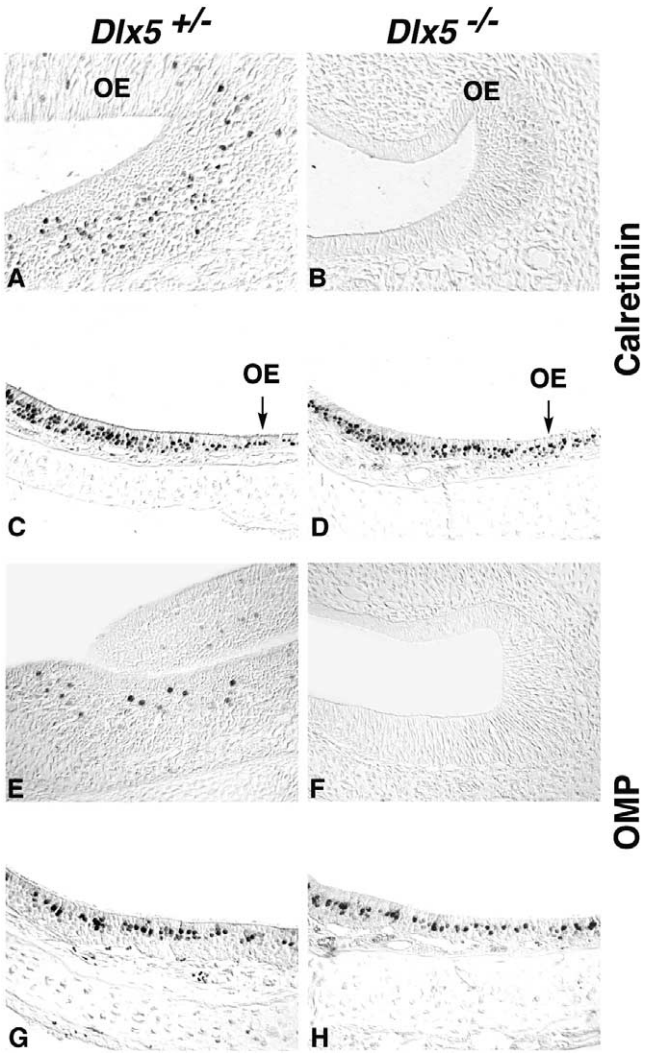

Fig. 2. Olfactory receptor neurons in $Dlx5^{-/-}$ mice. Characterization of ORN in the OE was done by immunohistochemistry with specific ORN markers. (A,B,E,F) Pictures from horizontal sections of E14.5 embryos, with the nasal cavity on the left, and the brain on the right. (C,D,G,H) Pictures from frontal sections of P0 animals. (A–D) Immunostaining for calretinin; (E–H) immunostaining for OMP. Sections from normal (left) and $Dlx5^{-/-}$ (right) animals are compared in each case. Note the absence of staining for calretinin or OMP in the $Dlx5^{-/-}$ OE at E14.5.

reach the mesenchymal region in the proximity of the forebrain meninges.

Dlx5 expression in the developing olfactory bulbs

Dlx5 is expressed in anterior and basal regions of the developing forebrain, including the OB, the rostral migratory stream (RMS), and the basal ganglia (Figs. 4A, 4C, 4C′, 4C″) (Acampora et al., 1999; Eisenstat et al., 1999; Simeone et al., 1994). We have extended this analysis to examine mice between E10.5 and P0, with special regard to late embryonic development. Staining for β-gal, in situ hybridization with *LacZ* in $Dlx5^{+/-}$ mice or in situ hybridization for *Dlx5* and *Dlx6* yielded the same distribution. At E16.5, *Dlx5* is expressed in the OB in cells located throughout the ventricular and granule layers, which contain primarily immature neurons and the soma of radial glia (Fig. 4J). The ventricular expression persists between E17.5 and P0. At P0, *Dlx5* is also found to be expressed in a cell layer external to the mitral/tufted cell layer of the OB, comprising the juxtaglomerular neurons (JGNs) (Figs. 4C, 4C′, 4C″). Immunostaining for β-gal on sections of $Dlx5^{+/-}$ OBs confirms the expression in granule layers and JGNs (Fig. 4E). Mitral/tufted cells do not express *Dlx5*, as no X-gal staining can be detected in this layer. However, expression in immature mitral/tufted cells prior to their forming a specific recognizable layer cannot be excluded. At P0 strong *Dlx5* expression is also present throughout the RMS (Fig. 4C). Interestingly, the accessory OB (AOB) does not express *Dlx5* at any stage examined (Figs. 4C″, 4D″, 5F). Consistently, in *Dlx5* null mice the AOB shows only minor defects (see following sections).

Olfactory bulb defects in Dlx5 null mice

$Dlx5^{-/-}$ OBs are approximately 30–50% smaller than normal OBs (Figs. 4B, 4D). Cells that would normally express *Dlx5* can be identified in mutant embryos by expression of the *LacZ* reporter gene. In normal embryos at E15.5–E16.5 these cells reside only in the ventricular and granule cell layers, while in newborn animals they are found in the granule and periglomerular layers. In *Dlx5* null mice, β-gal-positive cells are present throughout the OB while a proper mitral/tufted cell layer cannot be histologically recognized (Figs. 4D, 4D′, 4D″, 4F, 4K). The spread of *Dlx5*-expressing cells throughout the OB suggests a gross laminar organization defect. Despite the reduced OB size, the presence of the *Dlx5* cell lineage could be confirmed by X-gal staining and by in situ hybridization with either *LacZ* or *Dlx6* probes (not shown).

The absence of an evident mitral/tufted cell layer in *Dlx5* null OBs could result from a failure of migration of the precursor of JGNs or, alternatively, could reflect the loss of mitral cells or their dispersion in the OB. To answer this question, we have used two classic markers for the mitral/tufted cells: *Tbr1* and *reelin* (Alcantara et al., 1998; Bulfone et al., 1998; Schiffmann et al., 1997). Expression of these genes is specific for mitral/tufted cells during embryo development and in the adult. In situ hybridization with these probes yielded the same staining pattern; thus, only *reelin* is shown (Figs. 4E–4F′). In normal mice *reelin* signal is found in a single layer of the OB, corresponding to the location of mitral/tufted cells (Figs. 1E, 1E′). In contrast, in the $Dlx5^{-/-}$ brains signal is found in a wider and more irregular layer (Figs. 4G′–4H′). This result indicates that while mitral/tufted cells are clearly present in the mutant OB, they are dispersed over a much wider region.

To determine whether *Dlx5* inactivation affects the number of specific subpopulations of OB interneurons, we ex-

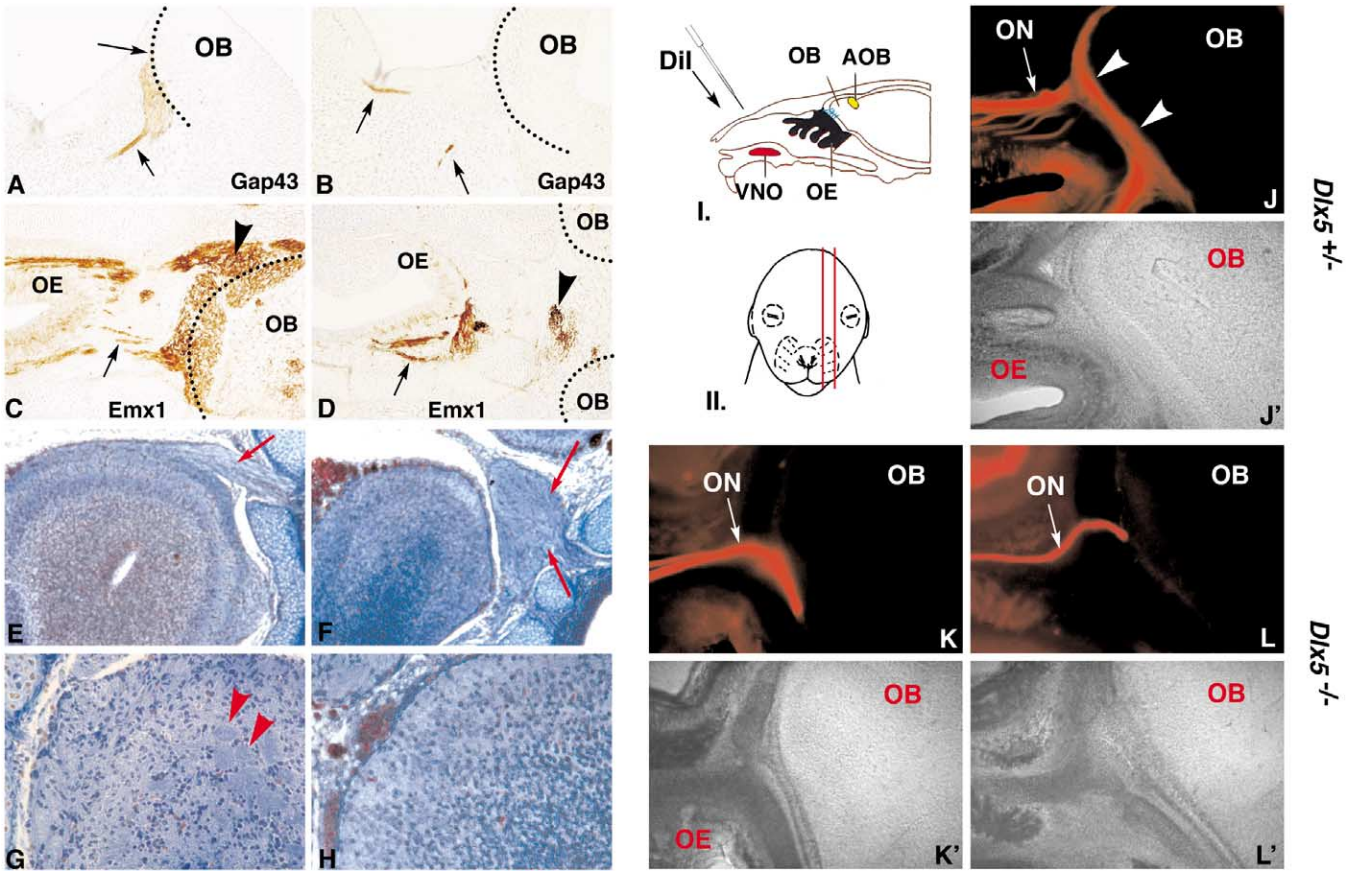

Fig. 3. Absence of olfactory connection in *Dlx5*$^{-/-}$ mice. (A,B) Longitudinal sections of E12.5 normal (A) and *Dlx5*$^{-/-}$ (B) embryos through the nasal mesenchyme and the anterior forebrain, stained for GAP43. Serial sections were examined. While in the normal embryos the nerve bundles reach the OB (black arrows), in the mutant embryos few GAP43-stained neurites can be seen (black arrows) but never in contact with the OB. (C,D) Horizontal sections of E14.5 normal (C) and *Dlx5*$^{-/-}$ (D) embryos stained for Emx1. Bundles of olfactory fibers (black arrows) can be seen, but these fail to form a neuropil (black arrowheads) or contact the OBs (sketched with black dotted lines). (E–H) Mallory staining of frontal sections of newborn normal (E,G) and *Dlx5*$^{-/-}$ (F,H) heads at lower (E,F) and higher (G,H) magnification. ORN fibers crossing the lamina cribrosa (red arrows) can be seen in both cases. In the *Dlx5*$^{-/-}$ contact with the OB is never observed. Glomeruli (red arrowheads) are visible in the normal OB (G) but absent in the *Dlx5*$^{-/-}$ (H). (J–L′) Tracing of the olfactory nerve with DiI. E16.5 embryos were injected with DiI and sectioned serially as illustrated (I. and II.). Normal (J) and *Dlx5*$^{-/-}$ (K,L) heads are shown. The olfactory and vomeronasal nerves are clearly visible in all cases (white arrows). The external nerve layer and the neuropil of the OB (white arrowheads) are visible in the normal OB but not in any of the mutant heads analyzed. For each fluorescent image (above), the corresponding bright-field image is shown below (J′, K′, L′). AOB, accessory olfactory bulb; OE, olfactory epithelium; ON, olfactory nerve; VNO, vomeronasal organ.

amined dopaminergic and GABAergic cells (Kosaka et al., 1995) by expression of tyrosine hydroxylase (TH) and glutamic acid decarboxylase (GAD67, Esclapez et al., 1994), respectively. In a normal OB, cells expressing these markers are expected in the periglomerular and the external granule cell layers. TH- and GAD67-immunoreactive cell bodies and neurites were detected in the periglomerular layer and there are abundant GAD67-positive cells and neurites in the outer granule cell layer, adjacent to the mitral/tufted cell layer (representing more mature granule cells) (Figs. 5A, 5C). Combined detection of β-gal (X-gal) and TH (anti-TH) on the same sections showed coexpression of these molecules (Figs. 5C, 5E), an indication that TH-immunoreactive JGNs are a subpopulation of *Dlx5*-expressing cells. In *Dlx5*$^{-/-}$ OBs TH- and GAD67-positive cells were either absent or greatly reduced in number (Figs. 5B, 5D), with no consistent distribution of the few remaining cells in any part of the OB. Double staining for β-gal and TH confirms that few or no *Dlx5/LacZ*-expressing cells also express TH (Fig. 5D) and that, conversely, TH-immunoreactive cells are easily detected in the AOB, where *Dlx5* is not expressed (Fig. 5F).

The lack of specific JGN populations could be due to the absence of these cells or to failure of these genes to be expressed in the mutant OB. Both the knock-in reporter *LacZ* and *Dlx6* are strongly expressed in the mutant OB; furthermore, β-gal-immunoreactive cells can be found throughout the thickness of the OB. Thus, the failure of expression of the differentiated markers TH and GAD67 is the more probable explanation, although this statement cannot be conclusively proven in the absence of an early JGN marker. In the AOB both TH- and GAD67-immunoreactive neurons were present, consistent with the absence of *Dlx5* expression in this region (Figs. 5A–5D). Their abnormal

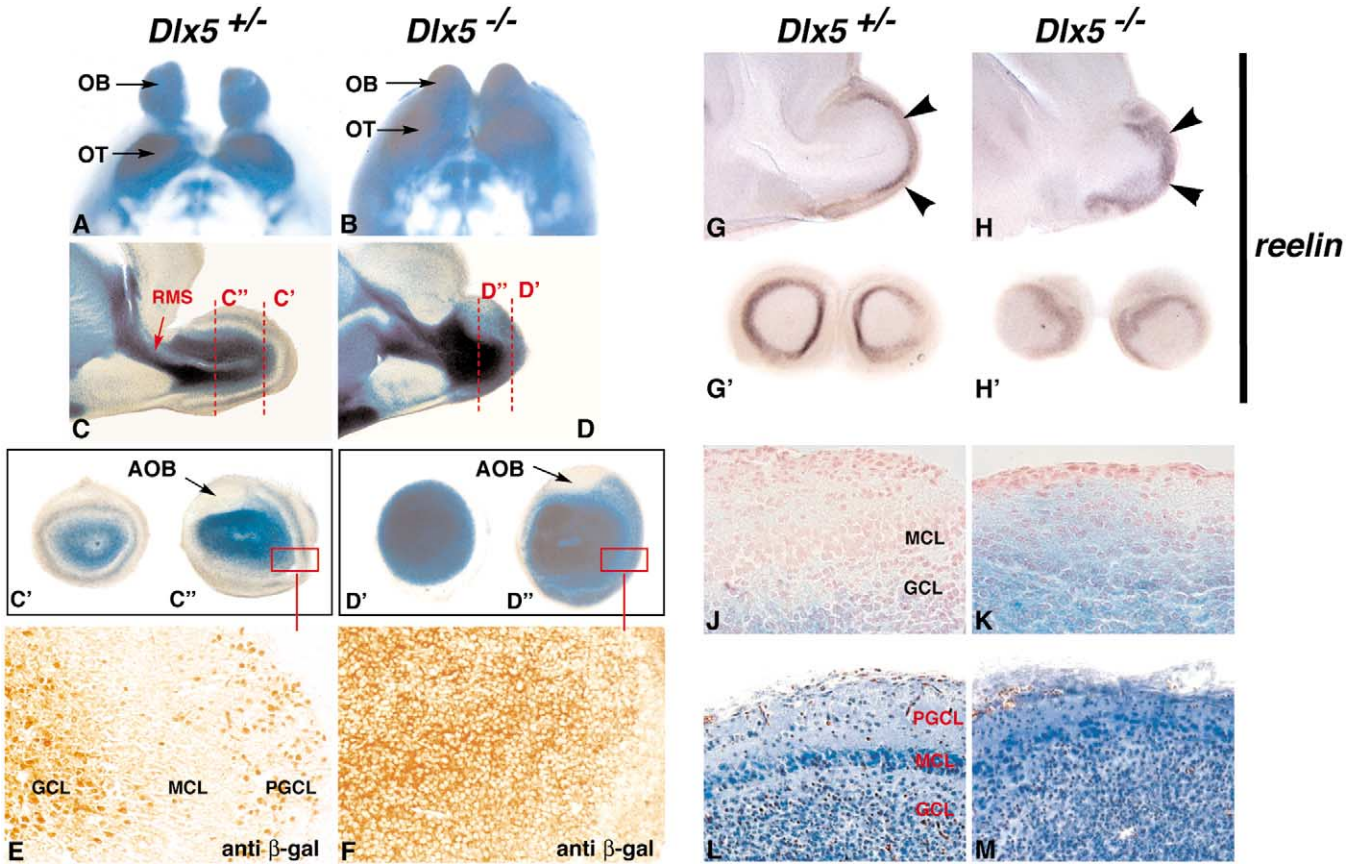

Fig. 4. Olfactory bulbs of normal and *Dlx5*$^{-/-}$ mice. (A,B) Newborn *Dlx5*$^{+/-}$ (A) and *Dlx5*$^{-/-}$ (B) brains, whole-mount stained for *LacZ* expression, ventral view. (C,D) Longitudinal thick sections from newborn *Dlx5*$^{+/-}$ (C) and *Dlx5*$^{-/-}$ (D) brains, stained with X-gal. (C′,C″,D′,D″) Frontal sections from newborn *Dlx5*$^{+/-}$ (C′,C″) and *Dlx5*$^{-/-}$ (D′,D″) brains. The sectioning level is indicated in (C) and (D) (dashed red, lines). (E,F) Immunohistochemistry for β-gal on frontal sections of *Dlx5*$^{+/-}$ (E) and *Dlx5*$^{-/-}$ (F) OB at P0, corresponding to the sketched areas (C″,D″ squares). Cell layers are indicated. (G–H′) In situ hybridization with *reelin* (marker for mitral/tufted cells, black arrowheads) on sections from newborn normal (G,G′) or *Dlx5*$^{-/-}$ (H,H′) brains, in longitudinal (G,H) or frontal (G′,H′) views. (J–M) Histology of OBs of *Dlx5*$^{+/-}$ (J,L) and *Dlx5*$^{-/-}$ (K,M) mice. (J,K) Sections from E16.5 embryos are stained with X-gal and counterstained with eosin. *LacZ* expression is found in the ventricular-granule cell layer. In the *Dlx5*$^{-/-}$ OB, no mitral/tufted cell layer can be identified. (L,M) Mallory's trichromic staining was performed on sections of newborn OBs. Note in the mutant OB the lack of typical lamination and of glomeruli. Cell layers are indicated. AOB, accessory olfactory bulb; GCL, granule cell layer; MCL, mitral/tufted cell layer; OB, olfactory bulb; OT, olfactory tubercle; PGCL, periglomerular cell layer; RMS, rostral migratory stream.

distribution is likely to be secondary to the lack of innervation.

Mitral/tufted cells was also examined for calretinin expression. In a normal OB, calretinin immunostaining is expected to reveal the nerve layer, a subpopulation of JGNs and of mitral/tufted cells (Malz et al., 2000; Wouterlood and Hrtig, 1995). While in the normal OB the expected immunoreactivity was observed, in *Dlx5*$^{-/-}$ OBs, no calretinin can be detected in the nerve layer or in any of the cell types (Figs. 5J, 5K). On the contrary, in the AOB calretinin-immunoreactive mitral/tufted cells were detected equally in the normal and the *Dlx5*$^{-/-}$ specimens (Figs. 5E, 5F, insets). The lack of calretinin expression in (*Dlx5* negative) mitral/tufted cells of *Dlx5*$^{-/-}$ OBs is likely to be secondary to a general OB lamination defect that disrupts the normal cell architecture.

The organization of the radial glia within the OB of normal and *Dlx5* null mice was investigated at P0 with the RC2 antibody, which recognizes an antigen expressed by radial glia throughout the brain. In normal OBs, RC2-positive glial fibers can be seen in the outer layer (Bailey et al., 1999; Puche and Shipley, 2001). In *Dlx5*$^{-/-}$ OBs, RC2-positive glial fibers are present in the OB but are less numerous, thinner, and disorganized compared with normal (data not shown).

Transplanted OBs from Dlx5$^{-/-}$ *mice can be innervated by wild-type ORNs*

The misrouting of ORN axons in *Dlx5* null animals could be due to defects in pathfinding/target recognition by the axons themselves and/or disruption of molecules in the OB essential for axon innervation. Specifically the OBs of the mutant mice may lack an attractive cue or overexpress a repulsive cue, resulting in disorganization of the axon trajectory. Furthermore, the marked downregulation of TH and

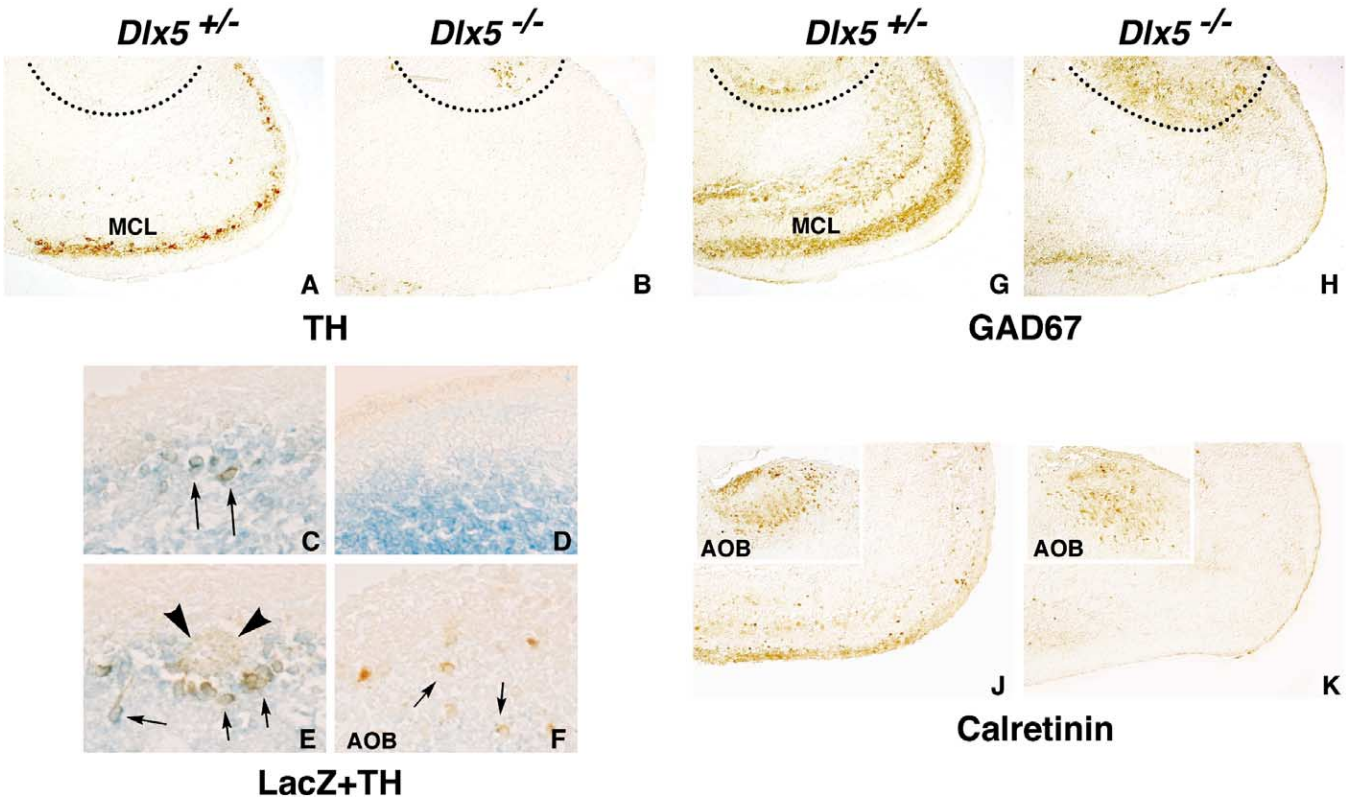

Fig. 5. Characterization of *Dlx5*$^{-/-}$ olfactory bulbs. Histochemistry with neuronal markers on sagittal OB sections. Panels on the left show normal (Dlx5$^{+/-}$) and panels on the right show mutant (Dlx5$^{-/-}$) OBs. Antigens detected are indicated on the bottom: (A,B) tyrosine hydroxylase TH; (C–F) X-gal staining (blue) followed by TH immunohistochemistry (brown); (G,H) glutamic acid decarboxylase GAD67; (J,K) calretinin. The AOB in (A), (B), (G), and (H) are sketched with black dotted lines. Inserts in (J) and (K) show calretinin immunostaining in the AOB. (C–F) Higher magnification of double staining for *Dlx5/LacZ* and TH, to show in the *Dlx5*$^{+/-}$ coexpression in the same JGN cells (black arrows). In (E) a glomerulus is observed surrounded by double-stained cells (arrowheads). In *Dlx5*$^{-/-}$ OBs, *LacZ*-positive cells did not show any TH immunoreactivity (D), while TH-immunoreactive, β-gal-negative cells (black, arrows) can be demonstrated in the AOB (F).

GAD67 expression in the mutant OBs might be the consequence of lack of connectivity (Kosaka et al., 1997; Stone et al., 1991). To address these issues we used an OB transplant paradigm. One OB from a wild-type newborn mouse was surgically removed and either an E16.5 or E18.5 *Dlx5*$^{-/-}$ donor OB transplanted into the vacant cavity. OBs from heterozygous *Dlx5/LacZ* mice were transplanted, as controls. The origin of the transplanted tissue was demonstrated by polymerase chain reaction (PCR) amplification of the *LacZ* transgene in DNA samples extracted from tissue sections adjacent to those analyzed by immunostaining, using DNA from the adjacent host forebrain as negative control (Fig. 6A). Further confirmation is provided by the appearance of the dissected whole brain (Figs. 6B, 6C), and by the overall organization and immunoreactivity of cell types (Figs. 6D–6O). This is to rule out that an outgrowth of CNS tissue may have taken the place of the surgically removed OB and be innervated by ORN neurites (Morrison and Graziadei, 1996).

Control (*Dlx5*$^{+/-}$ donor OB) and mutant (*Dlx5*$^{-/-}$ donor OB) transplants were approximately 50 and 30% the size of a normal bulb, respectively (Figs. 6B, 6C). In control transplanted OBs, abundant innervation of the transplanted tissue occurs. ORN axons enter the transplanted bulb and form glomeruli across the ventral, lateral, and medial surfaces. Similarly to a normal OB, dendrites from mitral/tufted cells and processes from astrocytes also participate in the formation of these glomeruli, as indicated by the double immunostaining for OMP/MAP2 and OMP/GFAP (Figs. 6D, 6E, 6G, 6H), although there looked to be fewer MAP2-positive dendrites penetrating the glomeruli of the *Dlx5*$^{-/-}$ OB. These glomeruli are surrounded by GAD67-positive and TH-positive JGNs (Figs. 6J, 6K, 6M, 6N), as expected. The expression of TH, which is dependent on, and modulated by, ORN activity and glutamate release (Baker et al., 1993; Puche and Shipley, 1999), indicates that the wild-type axons make functional connections to the transplanted normal bulb. In transplants of *Dlx5*$^{-/-}$ OBs the laminar disorganization seen in intact bulbs is also present in the transplanted tissue. Neurites from the host ORNs innervate the mutant OB and form glomeruli (Figs. 6F, 6I). These glomeruli are often smaller than those found in the control transplant. Double immunofluorescence on the *Dlx5*$^{-/-}$ transplanted bulbs also reveals OB dendrites (MAP2-positive) and bulb astrocyte (GFAP-positive) processes participating in the formation of glomeruli (Figs. 6F, 6I). However, there is a

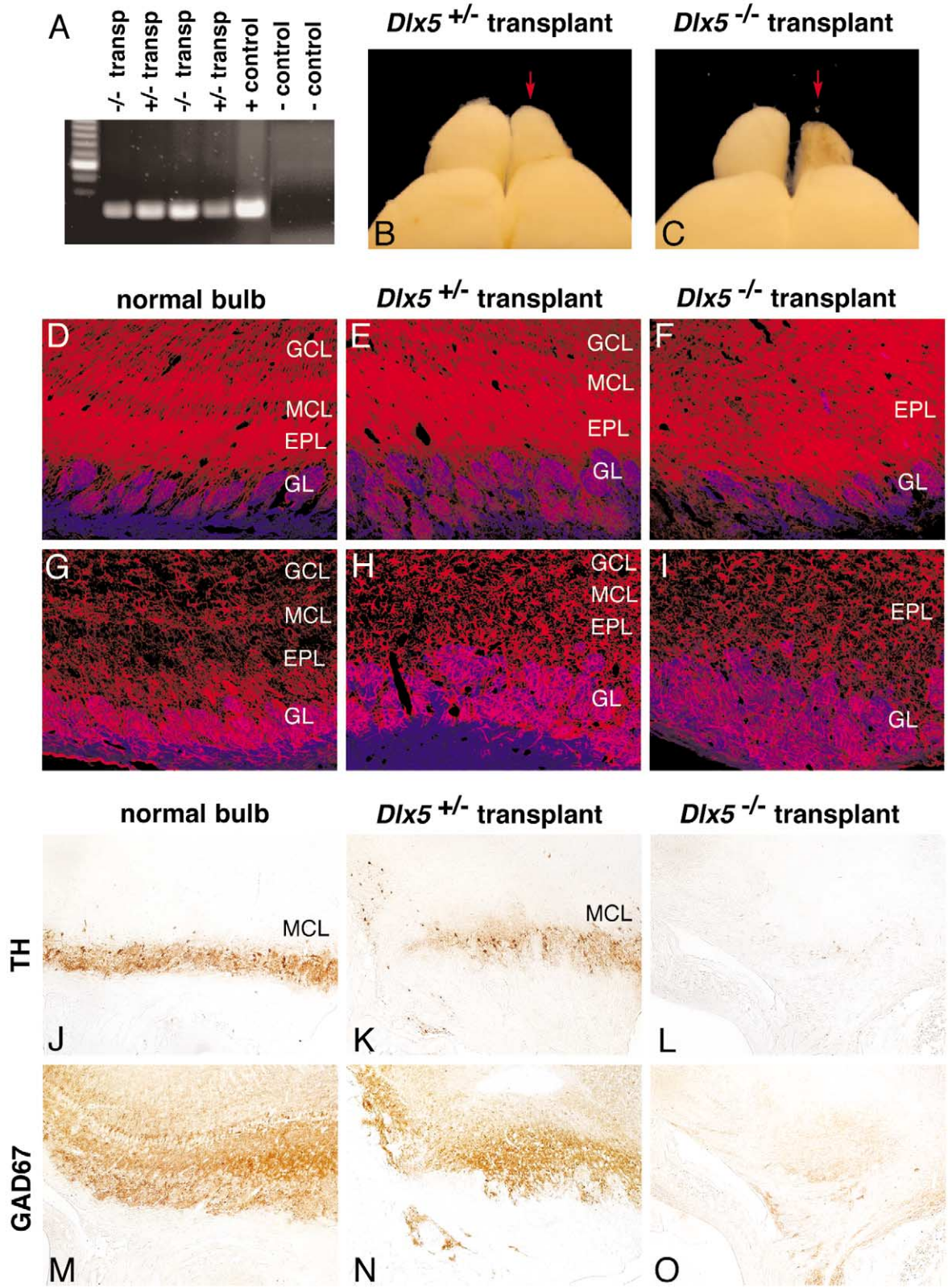

Fig. 6. Analysis of transplanted olfactory bulbs. A PCR amplification of *LacZ* sequences from genomic DNAs extracted from transplanted tissue (−/− or +/−). Negative controls are DNAs extracted from host forebrain tissue, positive control is DNA from +/− embryo. (B,C) Whole brain showing the transplanted normal (B) and $Dlx5^{-/-}$ (C) OBs (red arrows). The brown color on the $Dlx5^{-/-}$ transplant (C) marks blood vessels associated with the pia that could not be removed during dissection. (D–I) Double immunofluorescence on sections from nonoperated (D,G), control $Dlx5^{+/-}$ (E,H), and $Dlx5^{-/-}$ transplanted OBs (F,I) for OMP (blue) and either MAP2 (red, D–F) or GFAP (red, G–I), observed by confocal microscopy. Purple color at the glomerular layer indicates coexpression of these markers. The cell layers of the OBs are indicated on the right side of each panel. (J–O) Immunohistochemistry on longitudinal section of nonoperated (J,M), control transplanted (K,N), and $Dlx5^{-/-}$ transplanted (L,O) OBs. For each case TH and GAD67 immunostaining is shown. EPL, external plexiform layer; GCL, granule cell layer; GL, glomeruli; all other abbreviations as in previous figures.

reduction in the number and extension of MAP2-labeled processes, consistent with a reduction in interneuron populations in the transplanted bulbs.

To further characterize the transplanted *Dlx5*$^{-/-}$ OBs, sections were stained for GAD67 and TH. There is a near-complete absence of GAD67- and TH-positive neutrons in the transplanted *Dlx5*$^{-/-}$ OBs, much alike the whole-animal *Dlx5*$^{-/-}$ OB, whereas in the control transplant bulb these cells are present (Figs. 6L, 6O). Thus, the presence of wild-type axons forming glomeruli does not restore proper cell layering or expression of TH and GAD67 in the *Dlx5* mutant OBs. Further, the lack of dopaminergic and GABAergic cells in the whole animal is not due to simply the lack of ORN innervation. Taken together, these results indicate that a *Dlx5*$^{-/-}$ OB can be innervated by ORN axons, and thus the lack of ORN connection is the *Dlx5*$^{-/-}$ mice is likely due to changes in the ORNs or bridging mesenchyme rather than changes in the OB.

Discussion

The *Dlx* family of transcription factors is involved in controlling neurodevelopmental processes in vertebrates. In the OB *Dlx1* and *Dlx2* play a role in the formation of GABAergic and dopaminergic JGNs (Anderson et al., 1997; Bulfone et al., 1998). In this study, we show that *Dlx5* is required for establishment of the OB cytoarchitecture, JGN differentiation, and ORN axon target recognition/pathfinding.

Induction of the olfactory bulb

OB induction has been difficult to study due to inaccessibility of the embryonic olfactory system. Anatomical studies indicate that there is a population of early ORN axons that penetrate through the forebrain into the ventricular zone (Gong and Shipley, 1995; Santacana et al., 1992), and were hypothesized to play an inductive role in the formation of the OB. However, examinations of the developmental phenotype in *Emx2* and *Dlx5* null mice argue against an axon induction hypothesis. In *Emx2* mutant mice both the OE and OB are present but no axonal contact between these structures is found (Yoshida et al., 1997). Thus, the olfactory phenotypes of *Emx2* and *Dlx5* null mice are similar. However, the presence of any early transient axonal connections in these mice was not reported. If the axon induction hypothesis is correct these axons would arrive early to trigger OB development, independently of later-arriving axons. In *Dlx5* mutants, the absence of axonal connections between the OE and the OB is similar to that seen in the *Emx2* mutants. At the embryonic stages examined (E12–E19) we saw no evidence for ORNs contacting the OBs. Taken together, the olfactory defects seen in these mutant mice suggest that ON connections are not needed for induction of the OB and for specification of its major cell types.

A candidate tissue for an indirect inductive signal to trigger OB development is the mesenchyme. Recently, LaMantia (2000) showed that mesenchyme-to-OE induction occurs in the olfactory system and is mediated by retinoic acid (RA), FGF8, sonic hedgehog (shh), and BMP4. On the other side, OE and mesenchyme-to-forebrain, or just mesenchyme-to-forebrain, signals may underlie the induction of the OB, although such a mechanism has yet to be demonstrated. Experimental models involving *shh* inactivation (Chiang et al., 1996), RA teratogenesis (LaMantia et al., 1993), and disruption of *Pax6* (Dellovade et al., 1998) all lead to severely compromised OE and OB. In these models disruption to the OE is always associated with OB defects, consistent with signaling between these structures.

Dlx5 and cell differentiation in the olfactory bulb

Dlx genes play a role in cell migration and differentiation in defined brain regions. Disruption of *Dlx2* results in the failure of OB JGNs to express the dopaminergic phenotype (Qiu et al., 1995). The combined disruption of *Dlx1* and *Dlx2* results in multiple brain phenotypes, among which are the absence of GABAergic and dopaminergic JGNs in the OB, defects of the GABAergic neurons in the striatum, and impaired cell migration from the basal ganglia into the neocortex and hippocampus (Marin et al., 2000; Pleasure et al., 2000). The disruption of JGN formation in *Dlx1*/*Dlx2* mutant OBs is only qualitatively similar to the observed *Dlx5* phenotype: the first results in a total elimination of GABAergic cells, while *Dlx5* mutation results in a dramatic reduction in their number. In addition, disruption of *Dlx5* has profound effects on ORN axon guidance, whereas the *Dlx1* and *Dlx2* mutations do not. ORN axons expressing the P2 ORG sort and target a region of the *Dlx1*/*Dlx2* mutant OB in an apparently normal position (Bulfone et al., 1998). Thus, while several of the phenotypes caused by *Dlx1*/*Dlx2* and *Dlx5* disruption in the OB are similar, there are substantial differences in ORN axon growth.

In the *Dlx5*$^{-/-}$ OB, cellular organization and GABAergic/dopaminergic JGN differentiation are compromised. The expression of TH in the olfactory system is known to depend on activity from the olfactory nerve via glutamate (Baker et al 1993; Puche and Shipley, 1999), whereas the GABAergic phenotype in the OB is independent of neural input. The reduction in GABAergic/dopaminergic JGN numbers in the *Dlx5* mutant brain could not be rescued when a mutant bulb is innervated by normal ORN axons. Thus, the JGN disorganization and scarcity in *Dlx5* null animals are likely the result of the gene disruption and not a consequence of the lack of ORN axon input. Consistent with an intrinsic *Dlx5* function in the OB, *Dlx5* is expressed throughout the ventricular layer in early embryos, and in the subventricular, granule, and periglomerular layers at birth. In *Dlx5* null animals the numbers of proliferating cells and cells undergoing apoptosis were similar to normal; thus, the reduction of GABAergic/dopaminergic JGNs is unlikely to

be the result of a proliferative defect. We hypothesize that *Dlx5* is important for the migration and/or differentiation of OB immature JGNs. Consistent with this hypothesis, laminar disorganization and low expression of the differentiated cell marker calretinin were observed in the mutant OBs.

The phenotypic similarity between various *Dlx* null mice suggests that they may control different steps of the differentiation in the same cell lineage, as shown in the basal ganglia (Eisenstat et al., 1999; Marin et al., 2000). The absence of GABAergic JGNs in the *Dlx1*/*Dlx2* null OB compared with their incomplete absence in the *Dlx5* null suggests that *Dlx1*/*Dlx2* genes might be upstream of *Dlx5* in the OB and may participate in a transcriptional cascade, as shown during early forebrain development (Zerucha et al., 2000). Alternatively, we can postulate that *Dlx* genes are mutually regulated via homo- and heterodimerization with common partners, such as Msx and Dlxin (Masuda et al., 2001; Zhang et al., 1997).

Role of Dlx5 in olfactory axon pathfinding

How ORN axons navigate through the mesenchyme to their target is still poorly understood. Throughout development and in the adult, the olfactory system is dynamically maintained by controlled cell turnover and axon regeneration: new ORNs are born, extend axons to the OB, form topographic connections. The interest in elucidating these mechanisms is in their potential exploitation in neuronal regeneration of other areas of the CNS. The first axonal contact occurs at approximately E12 in mouse. Mature connections, however, develop around E19–P0 with the formation of glomeruli and expression of synaptic vesicle-associated proteins (Bailey et al., 1999; Puche and Shipley, 2001; Treloar et al., 1999). ORN axons reach the OB, penetrate, and form glomeruli via complex cellular and molecular interactions, still under investigation. For example, semaphorins and their neuropilin receptors are expressed in subpopulations of ORNs and have well-characterized neurite outgrowth modulating effects on ORN axons (Kobayashi et al., 1997; Renzi et al., 2000; Schwarting et al., 2000; Walz et al., 2002; Williams-Hogarth et al., 2000).

Phenotypically, the OE and ORN axons of *Dlx5* null mice appear relatively normal; thus, it was not readily apparent whether the absence of axonal connection between the OE and the OB could be attributed to ORN or OB defects. In our transplantation model, normal ORN axons innervated a mutant OB, and were able to form glomeruli in which processes from mitral/tufted cells and astrocytes also participated. These findings indicate that the *Dlx5* null OB does not per se prevent axonal ingrowth. Rather, the absence of *Dlx5* in ORNs is likely to alter expression of molecules critical to target recognition and/or pathfinding. The identity of such downstream molecule(s) remains to be determined. Since no connection was observed also at earlier stages, the molecular pathway essential for pathfinding, altered in the *Dlx5* null mice, may involve molecules expressed in the nasal mesenchyme, as the transplantation experiments cannot formally rule out this possibility.

Formation of glomeruli

Glomeruli form relatively late in OB development (Bailey et al., 1999; Hinds, 1972), at nearly the same time as the migration of immature JGNs into the periglomerular layer. ORN axons, JGN dendrites, mitral/tufted apical dendrites, and astrocyte processes all contribute to the structure of mature glomeruli. The observation of specific OB phenotypes in targeted mutant mice is casting new light on the cell and molecular mechanisms of glomerulus formation: glomeruli form normally in mice deficient for *Tbr1*, lacking mitral/tufted cells (Bulfone et al., 1998), and in mice with a double *Dlx1*/*Dlx2* disruption, lacking GABAergic and dopaminergic JGNs (Bulfone et al., 1998). Thus, glomerulus formation is not dependent on the presence of these cell types. In transplants of *Dlx5* mutant OBs, wild-type axons form glomeruli in the mutant OB in which there are few dopaminergic or GABAergic interneurons. These findings support the hypothesis that JGNs are not required for glomerulus formation.

Experimental methods

Generation of Dlx5 null mice

Mice with targeted disruption of *Dlx5* have been reported (Acampora et al., 1999). The mutated allele consisted of a deletion of the first two exons (including the ATG start codon) and their replacement with the *LacZ* reporter gene. This modification provides a marker for the *Dlx5*-expressing cell lineage. The presence of the transgene did not alter *Dlx5* expression, since β-gal expression in $Dlx5^{+/-}$ embryos has always recapitulated known *Dlx5* expression patterns. Genotypes were determined by PCR amplification of the wild-type and mutant alleles, as described (Acampora et al., 1999). Since no defect has been observed in the $Dlx5^{+/-}$ animals, we refer to either wild-type or $Dlx5^{+/-}$ mice as "normal."

Tissue preparation

Embryos were collected at 24-h intervals between E8.5 and E18.5 of gestation (the day of the plug was designated E0.5), while pups were sacrificed on the day of birth (P0). Pregnant mice were anesthetized with Avertin (Sigma), and embryos were collected by cesarean section. E8.5–E15.5 embryos were immersion fixed in 4% PAF in 0.1 M phosphate buffer (PB, pH 7.4) for 1 h. Instead, E16.5 to P0 animals were perfused with 4% PAF. Following perfusion, embryos were decapitated, and the heads were fixed, paraffin embedded, and sectioned for immunohistochemistry. For vibratome sectioning, brains were dissected after perfusion,

fixed for additional 30 min, transferred to PBS, and sectioned immediately. For lipophilic dye tracing, perfused animals were decapitated and the samples were kept in 4% PAF until dye injection. For cryostatic sectioning, samples were washed in PBS, incubated in 30% sucrose solution for 24 h, transferred in OCT, frozen, and sectioned at 15 μm. The Institutional Animal Care Committee approved all the animal procedures.

Histology and histochemistry

Whole-mount X-gal staining of embryos was carried out for 16–24 h at 32°C, after a 15-min fixation in 4% PAF and several washes in PBS, as described (Acampora et al., 1999). Stained embryos were either clarified in benzyl benzoate:benzyl alcohol 2:1 or embedded in paraffin and sectioned at 10-μm thickness. Mallory's trichrome and Luxol blue histological staining was carried out according to standard procedures. Immunohistochemistry was done in Tris-buffered saline (Tris 50 mM, pH 7.6, NaCl 150 mM), using standard protocols. The following primary antibodies were used: mouse monoclonal anti-BrdU (1:50; Dako), rabbit anti-activated caspase 3 (CM1 antisera, 1:4000; Idun Pharmaceutical), rabbit anti-β-gal (1:5000; ICN Biomedical), rabbit anti-calretinin (1:1000; Chemicon), rabbit anti-tyrosine hydroxylase (TH, 1:2000; Chemicon), rabbit anti-glutamic acid decarboxylase 67 kDa (GAD67, 1:2000; Chemicon), goat anti-olfactory marker protein (OMP, 1:3000; courtesy of Dr. Frank Margolis, University of Maryland), mouse anti-growth-associated protein 43 monoclonal (GAP43, 1:75; Zymed), mouse anti-microtubule-associated protein 2 (MAP-2, 1:3000; Roche–Boehringer), mouse RC2 monoclonal IgM (1:200; developed by Dr. Miyuki Yamamoto, obtained from the Developmental Studies Hybridoma Bank, University of Iowa Department of Biological Sciences), rabbit anti-glial fibrillary acidic protein (GFAP, 1:5000; Dako), anti-S-100 (1/200; BioGenex), anti-laminin (Duband and Thiery, 1987) and rabbit anti-Emx1 (1:500; courtesy of Professor G. Corte, University of Genoa, Genoa, Italy). The antibodies for GnRH, MAP2, and RC2 were used on frozen sections, all the others on paraffin sections. Rabbit and goat antisera were revealed with goat anti-rabbit (EnVision+, Dako) and rabbit anti-goat (Rockland) peroxidase-conjugated secondary antibodies, respectively. Mouse monoclonal antibodies were revealed with the ARK Kit (Dako), according to the manufacturer's specifications. Peroxidase was developed with DAB (Dako).

For detection of proliferating cells, pregnant female mice were injected intraperitoneally with BrdU (30 μg/g body wt in 0.9% saline solution) three times, at 2-h intervals, and sacrificed 6 h after the first injection. Embryos were collected at E14.5 and P0.5, fixed overnight in 4% PAF in PB, rinsed in PBS, and paraffin embedded. Serial 10-μm longitudinal sections were collected and stained with anti-BrdU antibody. Apoptosis was detected in serial paraffin sections corresponding to the OE using the terminal uridine nick end labeling method (TUNEL-POD Kit; Roche), according to the manufacturer's instructions. For additional confirmation of apoptotic cell distribution, immunohistochemistry with CM1 anti-active caspase-3 antibody was also performed.

In situ hybridization and probes

Newborn pups were perfused with 4% PAF; the brains were dissected, postfixed 16 h, embedded in gelatin/albumin, and sectioned (100 μm) using a Leica vibratome. At least three brains of each genotype were analyzed with each probe, either in frontal or in longitudinal sections, following a procedure modified from Wilkinson (1992). Sections were bleached with H_2O_2 for 1 h, washed with PBS + 0.1% Tween 20 (PBT), treated with 10 μg/ml proteinase K for 15 min, blocked with 2 mg/ml glycines and postfixed with 4% PAF and 0.2% glutaraldehyde for 20 min. Prehybridization and hybridization (1 μg/ml of DIG-labeled cRNA probe) were done in a buffer containing 50% deionized formamide, 5× SSC pH 4.5, 1% SDS, 50 μg/ml heparin, and 50 μg/ml of yeast tRNA, at 70°C. After hybridization, sections were washed in 50% formamide, 5× SSC, pH 7.5, 1% SDS, then in 0.5 M NaCl, 10 mM Tris–HCl (pH 7.5) + Tween. Sections were then treated with 100 μg/ml RNase A in 0.5 M NaCl, 10 mM Tris–HCl (pH 7.5) + Tween for 30 min at 37°C, then washed with 50% formamide, 2× SSC, pH 7.5, + Tween for 10 min at 37°C. Signal was detected with alkaline phosphatase-conjugated anti-DIG Fab fragments (1:5000; Roche–Boehringer) in 100 mM NaCl, 100 mM Tris–HCl, pH 9.5, 50 mM $MgCl_2$ + Tween supplemented with 1% goat serum for 16 h at 22°C, followed by color development with NBT and BCIP.

DIG-labeled cRNA probes were synthesized by in vitro transcription (Promega) of linearized plasmid vectors containing the appropriate cDNA sequences. The probe for murine *Dlx5* was an 850-bp fragment including the entire coding region of *Dlx5*. Specificity of the probe was tested by hybridization on homozygous *Dlx5* null embryos, which yielded negligible background staining. The probe for murine *Dlx6* was a 370-bp cDNA fragment obtained by RT-PCR amplification from embryo RNA, and constitutes the partial exons 3 and 4 of the gene. This probe contains neither the homeodomain nor the di- and trinucleotide repeat sequences found in the cDNA (Pfeffer et al., 2001). The probe for *reelin* was a 710-bp cDNA fragment obtained from Dr. T. Curran (St. Jude Childrens Hospital, Memphis, TN, USA). The probe for *Tbr1* is a 260-bp cDNA fragment obtained from Dr. J. Rubenstein and Dr. A. Bulfone (Ireland Lab Developmental Neurobiology, San Francisco, CA, USA).

DiI nerve tracing

Normal, heterozygous, and homozygous mutant mouse embryos (E16.5 and E17.5) and newborn mice were perfused with 4% PAF, and stored in 4% PAF until used. DiI

(1,1′-dihexadecyl-3,3,3′-tetramethylindocarbocyanine perchlorate, 3 mg/ml in DMSO) solution was carefully injected into the nasal cavities of the each embryo using a 27-gauge needle under microscopic observation, followed immediately by sealing of the nasal cavities with 2% PAF/2% agarose. The tissue was protected from light and kept for 3–6 weeks in semisolid 2% PAF/1% agarose at room temperature. Serial 100- to 150-mm vibratome sections were cut in a sagittal plane (see Fig. 3) and examined by fluorescence microscopy.

Transplantation of the olfactory bulbs

Transplant experiments use donor tissue from one animal transferred into the cavity of a second animal of the same genetic strain. Donor OBs were collected from E16.5 embryos +/− and −/− for the *Dlx5/LacZ* allele. Quick X-gal staining on the remaining brain tissue distinguished the +/− and +/+ genotypes, both of which showed a normal phenotype. The genotype of the donor tissue was confirmed by PCR following the procedures. Donor OBs were maintained in ice-cold Leibovitz's L15 containing 50 μg/ml gentamicin. The host animal (P0.5) was anesthetized by hypothermia and placed into a head holder. An incision was made through the skin covering the skull and a flap of skull above the OB was removed to expose the OB. One bulb was removed by aspiration with a glass pipet. The donor bulb was placed into the empty cavity, the bone flap replaced, and the opening closed with microsutures. The entire surgical procedure from anesthesia to recovery required 15–20 min to perform. Each pup was monitored during recovery and following the surgery for signs of distress and checked daily thereafter. Four control (+/−) and three experimental (−/−) OBs were transplanted and analyzed, yielding similar results. The opposite transplant operation, i.e., the transfer of a normal OB into a $Dlx5^{-/-}$ animal, cannot be done due to postnatal lethality of the latter. Three weeks after surgery, the transplanted and sham-operated animals were perfused with 4% PAF in PB, postfixed for 4 h, decalcified with 10% EDTA for 24 h, washed in PBS, and either paraffin embedded or cryopreserved. Sagittal 8-μm serial sections were analyzed by immunohistochemistry for: OMP (marker for mature ORN axons), TH (marker for dopaminergic interneurons), GAD67 (marker for GABAergic interneurons), MAP-2 (marker for dendrites), and GFAP (marker for astrocytes).

Photomicroscopy

Photographs were taken with a digital photocamera on an Olympus AX70 microscope or a Fluo View personal confocal microscope (Olympus) fitted with krypton/argon lasers and filters for the detection of Cy2/Cy3/Cy5 fluorophores. The monochrome confocal digital images were pseudo-colored red (Cy3) or blue (Cy2/Cy5) in the FluoView confocal software. The images were then contrast balanced, color matched, and assembled into panels using Photoshop 5.5 (Adobe Systems Inc.) and QuarkXPress 4.0 (Pantone Calibrated). No additional digital image manipulation was carried out.

Acknowledgments

We are grateful to Dr. J.L.R. Rubenstein, Dr. A. Bulfone, Dr. T. Curran, Dr. G. Corte, and Dr. F. Margolis for sharing probes and reagents. We also thank Dr. Michael T. Shipley, Professor A. Fasolo, and Dr. P. Bovolin for their helpful criticism. G.L. is supported by Telethon-Italy (Project GP0218/01), FISM (Project 2000/R/41), CNR (Progetto Finalizzato Biotecnologie), and Ministero della Sanità. G.R.M. is recipient of a Career Award (03/cp) from Telethon-Italy. L.P. is recipient of fellowship from AIRC, Italy.

References

Acampora, D., Merlo, G., Paleari, L., Zerega, B., Mantero, S., Barbieri, O., Postiglione, M.P., Simeone, A., Levi, G., 1999. Craniofacial, vestibular and bone defects in mice lacking the *Distal-less*-related gene *Dlx5*. Development 126, 3795–3809.

Alcantara, S., Ruiz, M., D'Arcangelo, G., Ezan, F., de Lecea, L., Curran, T., Sotelo, C., Soriano, P., 1998. Regional and cellular patterns of *reelin* mRNA expression in the forebrain of the developing and adult mouse. J. Neurosci. 18, 7779–7799.

Anchan, R.M., Drake, D., Haines, C.F., Gerwe, E.A., LaMantia, A.S., 1997. Disruption of local retinoid-mediated gene expression accompanies abnormal development in the mammalian olfactory pathway. J. Comp. Neurol. 379, 171–184.

Anderson, S.A., Qiu, M., Bulfone, A., Eisenstat, D.D., Meneses, J., Pedersen, R., Rubestein, J.L.R., 1997. Mutations of the homeobox genes *Dlx-1* and *Dlx-2* disrupt the striatal subventricular zone and differentiation of late born striatal neurons. Neuron 19, 27–37.

Bailey, M.S., Puche, A.C., Shipley, M.T., 1999. Development of the olfactory bulb: evidence for glia–neuron interaction in glomerular formation. J. Comp. Neurol. 415, 423–448.

Baker, H., Morel, K., Stone, D., Maruniak, J., 1993. Adult naris closure profoundly reduces tyrosine hydroxylase expression in the mouse olfactory bulb. Brain Res. 614, 109–116.

Bastianelli, E., Pochet, R., 1994. Distribution of calmodulin, calbindin-D28k and calretinin among rat olfactory nerve bundles. Neurosci. Lett. 169, 223–226.

Briata, P., DiBlas, E., Gulisano, M., Mallamaci, A., Iannone, R., Boncinell, E., Corte, G., 1996. EMX1 homeoprotein is expressed in cell nuclei of the developing cerebral cortex and in the axons of the olfactory sensory neurons. Mech. Dev. 57, 169–180.

Brunjes, P.C., Fisher, M., Grainger, R., 1998. The small-eye mutation results in abnormalities in the lateral cortical migratory stream. Brain Res. Dev. Brain. Res. 110, 121–125.

Buck, L.B., 2000. The molecular architecture of odor and pheromone sensing in mammals. Cell 100, 611–618.

Bulfone, A., Kim, H.J., Puelles, L., Porteus, M.H., Grippo, J.F., Rubenstein, J.L., 1993a. The mouse *Dlx-2* (*Tes-1*) gene is expressed in spatially restricted domains of the forebrain, face and limbs in midgestation mouse embryos. Mech. Dev. 40, 129–140.

Bulfone, A., Puelles, L., Porteus, M.H., Frohman, M.A., Martin, G.R., Rubenstein, J.L.R., 1993b. Spatially restricted expression of *Dlx-1*, *Dlx-2* (*Tes-1*), *Gbx-2*, and *Wnt3* in the embryonic day 12.5 mouse

forebrain defines potentially transverse and longitudinal segmental boundaries. J. Neurosci. 13, 3155–3172.

Bulfone, A., Wang, F., Hevner, R., Anderson, S., Cutforth, T., Chen, S., Meneses, J., Pedersen, R., Axel, R., Rubenstein, J.L.R., 1998. An olfactory sensory map develops in the absence of normal projection neurons or GABAergic interneurons. Neuron 21, 1273–1282.

Chiang, C., Litingtung, Y., Lee, E., Young, K.E., Corden, J.L., Westphal, H., Beachy, P.A., 1996. Cyclopia and defective axial patterning in mice lacking Sonic hedgehog gene function. Nature 383, 407–413.

Chuau, M.I., Au, C., 1991. Olfactory Schwann cells are derived from precursor cells in the olfactory epithelium. J. Neurosci. Res. 29, 172–180.

Dellovade, T.L., Pfaff, D.W., Schwanzel-Fukuda, M., 1998. Olfactory bulb development is altered in small-eye (Sey) mice. J. Comp. Neurol. 402, 402–418.

Depew, M.J., Liu, J.K., Long, J.E., Presley, R., Meneses, J.J., Pedersen, R., Rubenstein, J.L.R., 1999. *Dlx5* regulates regional development of the branchial arches and sensory capsules. Development 126, 3831–3846.

Duband, J.L., Thiery, J.P., 1987. Distribution of laminin and collagens during avian neural crest development. Development 101, 461–478.

Eisenstat, D.D., Liu, J.K., Mione, M., Zhong, W., Yu, G., Anderson, S.A., Ghattas, I., Puelles, L., Rubenstein, J.L.R., 1999. DLX-1, DLX-2, and DLX-5 expression define distinct stages of basal forebrain differentiation. J. Comp. Neurol. 414, 217–237.

Esclapez, M., Tillakaratne, N.J.K., Kaufman, D.L., Tobin, A.J., Houser, C.R., 1994. Comparative localization of two forms of glutamic acid decarboxylase, and their mRNAs in rat brain supports the concept of functional differences between the forms. J. Neurosci. 14, 1834–1855.

Franz, T., 1994. Extra-toes (Xt) homozygous mutant mice demonstrate a role for the Gli-3 gene in the development of the forebrain. Acta Anat. (Basel) 150, 38–44.

Gad, J.M., Keeling, S.L., Wilks, A.F., Tan, S.S., Cooper, H.M., 1997. The expression patterns of guidance receptors, DCC and Neogenin, are spatially and temporally distinct throughout mouse embryogenesis. Dev. Biol. 192, 258–273.

Gao, P.P., Sun, C.H., Zhou, X.F., DiCicco-Bloom, E., Zhou, R., 2000. Ephrins stimulate or inhibit neurite outgrowth and survival as a function of neuronal cell type. J. Neurosci. Res. 60, 427–436.

Giger, R.J., Pasterkamp, R.J., Heijnen, S., Holtmaat, A.J., Verhaagen, J., 1998. Anatomical distribution of the chemorepellent semaphorin III/collapsin-1 in the adult rat and human brain: predominant expression in structures of the olfactory–hippocampal pathway and the motor system. J. Neurosci. Res. 52, 27–42.

Gong, Q., Shipley, M.T., 1995. Evidence that pioneer olfactory axons regulate telencephalon cell cycle kinetics to induce the formation of the olfactory bulb. Neuron 14, 91–101.

Gong, Q., Shipley, M.T., 1996. Expression of extracellular matrix molecules and cell surface molecules in the olfactory nerve pathway during early development. J. Comp. Neurol. 366, 1–14.

Hinds, J.W., 1972. Early neuron differentiation in the mouse olfactory bulb. I. Light microscopy. J. Comp. Neurol. 146, 233–252.

Keller, A., Margolis, F.L., 1975. Immunological studies of the rat olfactory marker protein. J. Neurochem. 24, 1101–1106.

Key, B., 1998. Molecular development of the olfactory nerve pathway. Ann. NY Acad. Sci. 855, 76–82.

Kobayashi, H., Koppel, A.M., Luo, Y., Raper, J.A., 1997. A role for collapsin-1 in olfactory and cranial sensory axon guidance. J. Neurosci. 17, 8339–8352.

Kosaka, K., Aika, Y., Toida, K., Heizmann, C.W., Hunziker, W., Jacobowitz, D.M., Nagatsu, I., Streit, P., Visser, T.J., Kosaka, T., 1995. Chemically defined neuron groups and their subpopulation in the glomerular layer of the rat main olfactory bulb. Neurosci. Res. 23, 73–88.

Kosaka, K., Fujii, M., Toida, K., Kosaka, T., 1997. Differentiation of chemically defined neuronal populations in the transplanted olfactory bulb without olfactory receptor innervation. Neurosci. Res. 28, 11–19.

LaMantia, A.S., Bhasin, N., Rhodes, K., Heemskerk, J., 2000. Mesenchymal/epithelial induction mediates olfactory pathway formation. Neuron 28, 411–425.

LaMantia, A.S., Colbert, M.C., Linney, E., 1993. Retinoic acid induction and regional differentiation prefigure olfactory pathway formation in the mammalian forebrain. Neuron 10, 1035–1048.

Li, H.S., Chen, J., Wu, W., Fagaly, T., Zhou, L., Yuan, W., Dupuis, S., Jiang, Z., Nash, W., Gick, C., Ornitz, D.M., Wu, J.Y., Rao, Y., 1999. Vertebrate slit, a secreted ligand for the transmembrane protein roundabout, is a repellent for olfactory bulb axons. Cell 96, 807–818.

Lin, D.M., Ngai, J., 1999. Development of the vertebrate main olfactory system. Curr. Opin. Neurobiol. 9, 74–78.

Liu, J.K., Ghattas, I., Liu, S., Chen, S., Rubenstein, J.L.R., 1997. *Dlx* genes encode DNA-binding proteins that are expressed in an overlapping and sequential pattern during basal ganglia differentiation. Dev. Dyn. 210, 498–512.

Lopez-Mascaraque, L., Garcia, C., Valverde, F., de Carlos, J.A., 1998. Central olfactory structures in *Pax6* mutant mice. Ann. NY Acad. Sci. 855, 83–94.

Malz, C.R., Knabe, W., Kuhn, H.J., 2000. Pattern of calretinin immunoreactivity in the main olfactory system and the vomeronasal system of the tree shrew, *Tupaia belangeri*. J. Comp. Neurol. 420, 428–436.

Margolis, F., 1972. A brain protein unique to the olfactory bulb. Proc. Natl. Acad. Sci. USA 69, 1221–1224.

Marin, O., Anderson, S.A., Rubenstein, J.L.R., 2000. Origin and molecular specification of striatal interneurons. J. Neurosci. 20, 6063–76.

Masuda, Y., Sasaki, A., Shibuya, H., Ueno, N., Ikeda, K., Watanabe, K., 2001. Dlxin-1, a novel protein that binds Dlx5 and regulates its transcriptional function. J. Biol. Chem. 276, 5331–5338.

Merlo, G.R., Zerega, B., Paleari, L., Trombino, S., Mantero, S., Levi, G., 2000. Multiple functions of *Dlx* genes. Int. J. Dev. Biol. 44, 619–626.

Mombaerts, P., Wang, F., Dulac, C., Chao, S.K., Nemes, A., Mendelshon, M., Edmondson, J., Axel, R., 1996. Visualizing an olfactory sensory map. Cell 87, 675–68.

Morrison, E.E., Graziadei, P.P., 1996. An ultrastructural study of glomeruli associated with vomeronasal organs transplanted into the rat CNS. Anat. Embryol. (Berlin) 193, 331–339.

Norgren Jr., R.B., Ratner, N., Brackenbury, R., 1992. Development of olfactory nerve glia defined by a monoclonal antibody specific for Schwann cells. Dev. Dyn. 194, 231–238.

Pasterkamp, R.J., Ruitenberg, M.J., Verhaagen, J., 1999. Semaphorins and their receptors in olfactory axon guidance. Cell. Mol. Biol. (Noisy-le-Grand) 45, 763–779.

Pfeffer, U., Ferro, P., Pavia, V., Trombino, S., Dell'Eva, R., Merlo, G.R., Levi, G., 2001. The coding region of the human DLX6 gene contains a polymorphic CAG/CCG repeat. Int. J. Oncol. 18, 1293–1297.

Pleasure, S.J., Anderson, S., Hevner, R., Bagri, A., Marin, O., Lowenstein, D.H., Rubenstein, J.L.R., 2000. Cell migration from the ganglionic eminences is required for the development of hippocampal GABAergic interneurons. Neuron 28, 727–40.

Porteus, M.H., Bulfone, A., Liu, J.K., Puelles, L., Lo, L.C., Rubenstein, J.L.R., 1994. DLX-2, MASH-1, MAP-2 expression and bromodeoxyuridine incorporation define molecularly distinct cell populations in the embryonic mouse forebrain. J. Neurosci. 14, 6370–6383.

Puche, A.C., Poirier, F., Hair, M., Bartlett, P.F., Key, B., 1996. Role of galectin-1 in the developing mouse olfactory system. Dev. Biol. 179, 274–287.

Puche, A.C., Shipley, M.T., 1999. Odor-induced, activity-dependent transneuronal gene induction in vitro: mediation by NMDA receptors. J. Neurosci. 19, 1359–1370.

Puche, A.C., Shipley, M.T., 2001. Radial glia development in the mouse olfactory bulb. J. Comp. Neurol. 434, 1–12.

Qiu, M., Bulfone, A., Ghattas, I., Meneses, J.J., Christensen, L., Sharpe, P.T., Presley, R., Pedersen, R.A., Rubenstein, J.L.R., 1997. Role of Dlx1 and Dlx2 in proximodistal patterning of the branchial arches: mutation of Dlx1, Dlx2, and Dlx1 + Dlx2 alter morphogenesis of

proximal elements derived from the first and second arches. Dev. Biol. 185, 165–184.

Qiu, M., Bulfone, A., Martinez, S., Meneses, J.J., Shimamura, K., Pedersen, R.A., Rubenstein, J.L.R., 1995. Null mutation of *Dlx-2* results in abnormal morphogenesis of proximal first and second branchial arch derivatives and abnormal differentiation of the forebrain. Genes Dev. 9, 2523–2538.

Ramon-Cueto, A., A vila, J., 1998. Olfactory ensheating glia: properties and function. Brain Res. Bull. 46, 175–187.

Renzi, M.J., Wexler, T.L., Raper, J.A., 2000. Olfactory sensory axons expressing a dominant-negative semaphorin receptor enter the CNS early and overshoot their target. Neuron 28, 437–447.

Robinson, G.W., Mahon, K.A., 1994. Differential and overlapping expression domains of Dlx2 and Dlx3 suggest distinct roles for *Distal-less* homeobox genes in craniofacial development. Mech. Dev. 48, 199–215.

Santacana, M., Heredia, M., Valverde, F., 1992. Transient pattern of exuberant projections of olfactory axons during development in the rat. Brain Res. Dev. Brain Res. 70, 213–222.

Schiffmann, S.N., Bernier, B., Gofinet, A.M., 1997. *Reelin* mRNA expression during mouse brain development. Eur. J. Neurosci. 9, 1055–1071.

Schimmang, T., Lemaistre, M., Vortkamp, A., Ruther, U., 1992. Expression of the zinc finger gene Gli3 is affected in the morphogenetic mouse mutant extra-toes (Xt). Development 116, 799–804.

Schwarting, G.A., Kostek, C., Ahmad, N., Dibble, C., Pays, L., Puschel, A.W., 2000. Semaphorin 3A is required for guidance of olfactory axons in mice. J. Neurosci. 20, 7691–7697.

Shu, T., Valentino, K.M., Seaman, C., Cooper, H.M., Richards, L.J., 2000. Expression of the netrin-1 receptor, deleted in colorectal cancer (DCC), is largely confined to projecting neurons in the developing forebrain. J. Comp. Neurol. 416, 201–212.

Simeone, A., Acampora, D., Pannese, M., D'Esposito, M., Stornaiuolo, A., Gulisano, M., Mallamaci, A., Kastury, K., Druck, T., Huebner, K., Boncinelli, E., 1994. Cloning and characterization of two members of the vertebrate *Dlx* gene family. Proc. Natl. Acad. Sci. USA 91, 2250–2254.

St. John, J.A., Tisay, K.T., Caras, I.W., Key, B., 2000. Expression of EphA5 during development of the olfactory nerve pathway in rat. J. Comp. Neurol. 416, 540–550.

Stone, D.M., Grillo, M., Margolis, F.L., Joh, T.H., Baker, H., 1991. Differential effect of functional olfactory bulb deafferentation on tyrosine hydroxylase and glutamic acid decarboxylase messanger RNA levels in rodent juxtaglomerular neurons. J. Comp. Neurol. 311, 223–233.

Tenne-Brown, J., Puche, A.C., Key, B., 1998. Expression of galectin-1 in the mouse olfactory system. Int. J. Dev. Biol. 42, 791–799.

Tisay, K.T., Bartlett, P.F., Key, B., 2000. Primary olfactory axons form ectopic glomeruli in mice lacking p75NTR. J. Comp. Neurol. 428, 656–670.

Treloar, H.B., Nurcombe, V., Key, B., 1996. Expression of extracellular matrix molecules in the embryonic rat olfactory pathway. J. Neurobiol. 31, 41–55.

Treloar, H.B., Purcell, A.L., Greer, C.A., 1999. Glomerular formation in the developing rat olfactory bulb. J. Comp. Neurol. 413, 289–304.

Treloar, H.B., Tomasiewicz, H., Magnuson, T., Key, B., 1997. The central pathway of primary olfactory axons is abnormal in mice lacking the N-CAM-180 isoform. J. Neurobiol. 32, 643–658.

Vassar, R., Chao, S.K., Sitcheran, R., Nunez, J.M., Vosshal, L.B., Axel, R., 1994. Topographic organization of sensory projections to the olfactory bulb. Cell 79, 981–991.

Walz, A., Rodriguez, I., Mombaerts, P., 2002. Aberrant sensory innervation of the olfactory bulb in neuropilin-2 mutant mice. J. Neurosci. 22, 4025–4035.

Wang, F., Nemes, A., Mendelsohn, M., Axel, R., 1998. Odorant receptors govern the formation of a precise topografic map. Cell 93, 47–60.

Wilkinson, D.G., 1992. Whole-mount in situ hybridization of vertebrate embryos, in: Wilkinson, D.G. (Ed.), In Situ Hybridization: A Practical Approach, IRL Press, Oxford, pp. 75–83.

Williams-Hogarth, L.C., Puche, A.C., Torrey, C., Cai, X., Song, I., Kolodkin, A.L., Shipley, M.T., Ronnett, G.V., 2000. Expression of semaphorins in developing and regenerating olfactory epithelium. J. Comp. Neurol. 423, 565–578.

Wouterlood, F.G., Hrtig, W., 1995. Calretinin-immunoreactivity in mitral cells of the rat olfactory bulb. Brain Res. 682, 93–100.

Wu, W., Wong, K., Chen, J., Jiang, Z., Dupuis, S., Wu, J.Y., Rao, Y., 1999. Directional guidance of neuronal migration in the olfactory system by the protein Slit. Nature 400, 331–336.

Yang, L., Zhang, H., Hu, G., Wand, H., Abate-Shen, C., Shen, M.M., 1998. An early phase of embryonic *Dlx5* expression defines the rostral boundary of the neural plate. J. Neurosci. 18, 8322–8330.

Yoshida, M., Suda, Y., Matsue, I., Miyamoto, N., Takeda, N., Kuratani, S., Aizawa, S., 1997. Emx1 and Emx2 functions in development of dorsal telencephalon. Development 124, 101–111.

Zerucha, T., Stuhmer, T., Hatch, G., Park, B.K., Long, Q., Yu, G., Gambarotta, A., Schultz, J.R., Rubenstein, J.L.R., Ekker, M., 2000. A highly conserved enhancer in the *Dlx5/Dlx6* intragenic region is the site of cross-regulatory interactions between *Dlx* genes in the embryonic forebrain. J. Neurosci. 20, 709–721.

Zhang, H., Hu, G., Wang, H., Sciavolino, P., Iler, N., Shen, M.M., Abate-Shen, C., 1997. Hetero-dimerization of Msx and Dlx homeoproteins results in functional antagonism. Mol. Cell Biol. 17, 2920–2932.